Spatial heterogeneity, terminus environment effects and acceleration in mass loss of glaciers and ice caps across Greenland

Michael Grimes, Jonathan L. Carrivick [*], Mark W. Smith

School of Geography and water@leeds, University of Leeds, Woodhouse Lane, Leeds LS2 9JT, UK

ARTICLE INFO

ABSTRACT

Greenland's peripheral glaciers and ice caps (GICs) contribute significant amounts of meltwater to the oceans but also affect local economies and livelihoods. Here we created multi-temporal geodetic elevation change datasets to compute mass changes for 6149 glaciers around the entire periphery of Greenland. These glaciers have lost a total of at least 276 ± 55 Gt of ice, or 0.76 ± 0.15 mm sea level equivalent, from their ablation areas between 1978 and 2015. If we assume no mass loss within accumulation areas, then the mean mass balance has been at least -0.10 ± 0.02 m w.e. yr^{-1}. In general, west Greenland glaciers have had a more negative mass balance and experienced accelerated mass loss since 2006 (x 2.7 in south west region, x 5.6 in central west region). Conversely, east Greenland glaciers have generally experienced a decrease in the rate of mass loss. Lake-terminating glaciers have experienced the most negative mass balance, exacerbated by the occurrence of debris cover. These findings quantify great spatial heterogeneity, give context to the recent history of mass loss from GICs, and suggest the importance of including local glacier properties within glacier evolution models.

1. Introduction

Global climate change is manifest in a warming trend and an increase in the magnitude and frequency of abrupt and disruptive climate shifts (Knox, 1993; Pittock, 2012; Russo et al., 2014). These climate shifts are occurring fastest in Arctic regions (Serreze and Barry, 2011; Zemp et al., 2015). Climate warming across the Arctic has been measured at double the global mean rate since the 1970s (Holland and Bitz, 2003; Chylek et al., 2009; Screen and Simmonds, 2010a, 2010b; Pithan and Maur-itsen, 2014). Within the Arctic, Greenland has experienced especially pronounced warming; from 2007 to 2012 air temperatures were 3° C higher than the 1979 to 2000 baseline global average (Mayewski et al., 2014). However, more recently the rate of warming has decreased with only a very slight rising trend since 2000 (Hanna et al., 2021).

Consequently, Greenland's peripheral glaciers and ice caps (GICs) are changing rapidly. GICs represent only ~5% of the ice-covered area of Greenland and equate to just ~0.5% of the volume of the Greenland Ice Sheet (GrIS) (Rastner et al., 2012), but they are three to four times more sensitive to ongoing atmospheric climate warming when compared to the Greenland Ice Sheet (GrIS) (Fettweis et al., 2008, 2013; Goelzer et al., 2013; Machguth et al., 2013). GICs contributed between 14% and 20% of the total ice loss from Greenland between October 2003 and March 2008 (Bjørk et al., 2012; Bolch et al., 2013). However, there is considerable regional variability in the absolute amount and rate of change of glacier mass loss across Greenland (Hugonnet et al., 2021; Khan et al., 2022).

Greenland GICs are presently contributing a disproportionately high volume of meltwater to surrounding oceans and to global sea level rise (Bintanja and Selten, 2014). The heightened sensitivity of GICs to atmospheric climate warming when compared to the GrIS is largely a function of: (i) predominantly terrestrial termini that are (more) sensitive to atmospheric warming (than marine termini that already have low basal friction); (ii) short reservoir times and faster mass turnover (Bolch et al., 2013; Bintanja and Selten, 2014); and (iii) smaller surface area (generally <5 km²) existing at elevations lower than the elevation of the majority of the GrIS (Raper and Braithwaite, 2006; Pfeffer et al., 2014; Bjørk et al., 2018). Locally, runoff from Greenland GICs affects fjord water quality and circulation, which has consequences for the primary production and marine ecosystems (Hopwood et al., 2020; Krisch et al., 2020).

Despite the disproportionate contribution of GICs to Greenland runoff and the societal importance of that runoff, previous studies examining geometric and mass changes of Greenland GICs have been either spatially- or temporally-restricted. Spatially-localised studies

---

include those for Holm Land (von Albedyll et al., 2018), northeast Greenland, for Disko Island in west Greenland between 1985 and 2015 (Huber et al., 2020), and for Prudhoe Land, northwest Greenland between 1985 and 2018 (Wang et al., 2021). Multi-regional studies of geodetic changes to Greenland GICs (Hugonnet et al., 2021; Khan et al., 2022) have to date been temporally-limited by the availability of suitable coverage satellite-derived elevation datasets; ASTER launched in 1999, SRTM launched in 2000, ICESat launched in 2003, TerraSAR-X launched in 2007, TanDEM-X launched in 2010, which mostly cover the last few decades only.

The aim of this study is therefore to determine GIC mass changes over a multi-decadal timescale. We will identify temporal trends, spatial patterns, glacier groups and anomalies, and thereby suggest controls on GIC mass loss, which is key to informing projections of GIC evolution.

2. Datasets and methods

2.1. DEM preparation and co-registration

In this study we use data from three multi-temporal digital elevation models (DEMs). We focus our reporting of our results on analyses using the earliest and the latest of these, which are the AeroDEM that was derived from aerial photographs acquired between 1978 and 1987, and the ArcticDEM that has a mean date of 2015 for Greenland.

AeroDEM reports a < 10 m horizontal and < 6 m vertical accuracy, which we address via co-registration as elaborated upon later in this section. In this study, AeroDEM elevation data, orthorectified 8-bit greyscale image files, and associated reliability mask (Korsgaard et al., 2016) were mosaiced based on their collection years (1978, 1981, 1985 and 1987; Fig. 1). AeroDEM elevation mosaics were resampled from 25 m to 30 m using a bilinear interpolation deemed most appropriate due to the relatively small change in resolution, relatively consistent and low slope angles on glacier surfaces at this resolution, and a lack of topographic complexity on glacier surfaces (Smith et al., 2004; Nuth and Kääb, 2011; Shi et al., 2014; Seehaus et al., 2020; McNabb et al., 2019a).

The ArcticDEM 2 m mosaic (Porter et al., 2023) is constructed from pairs of submeter resolution Maxar, WorldView and GeoEye images acquired between 2007 and 2022. ArcticDEM data is generated by applying stereo auto-correlation techniques to overlapping pairs of high-resolution optical satellite images using the Surface Extraction from TIN-based Searchspace Minimization (SETSM) software (Noh and Howat, 2015). When corrected to ICESat elevations the ArcticDEM has a vertical accuracy of ~0.1 m (Candela et al., 2017; Shiggins et al., 2023). In this study the ArcticDEM was re-sampled to 30 m using a bilinear interpolation (Seehaus et al., 2020).

Curious to try and detect changes within our ~40 year time period, we also processed and analysed the GIMP (Howat et al., 2015) DEM (v1, 30 m horizontal resolution). However, despite erroneous values having been filtered and filled (Xing et al., 2020), and whilst nominally pertaining to 2006, the GIMP DEM has an unspecified time range of images used in its construction. It also retains low accuracy. We therefore focus our results herein on changes between AeroDEM and ArcticDEM (1978 to 2015), and only cautiously consider the sub-periods of AeroDEM to GIMP and for GIMP to ArcticDEM, whilst remaining mindful of the higher uncertainties for these time periods.

All DEMs were projected to EPSG:5938 (WGS 84 / EPSG Greenland Polar Stereographic) and then clipped to the footprints dictated by the AeroDEM times of capture for co-registration. DEMs were coregistered per AeroDEM year area (Fig. 1) using the Nuth and Kääb (2011) method implemented in DEMcoreg (Shean et al., 2016; Beyer et al., 2018). Both the AeroDEM and GIMP DEMs were coregistered to ArcticDEM using a glacier mask derived from RGI v6.0 (RGI Consortium, 2017) to only consider non-glacier surfaces within the co-registration algorithms. Co-registering to the ArcticDEM maintains consistency of application and reduces the propagation of imprecision and inaccuracy which may be imparted by sequential co-registration. Results of co-registration are presented in our Supplementary Information.

2.2. Glacier outlines

Whilst we co-registered entire landscape-wide DEMs, the elevation change analysis herein only pertains to glacier surfaces. We used the RGI v6.0 outlines (RGI Consortium, 2017) which for the majority of GICs represent GIC extent in ~2001 as based on the inventory of Rastner et al. (2012), but north of ~81 ° N are based on Howat et al. (2014). Glaciers with a connectedness >1 (weak connection) were excluded from our
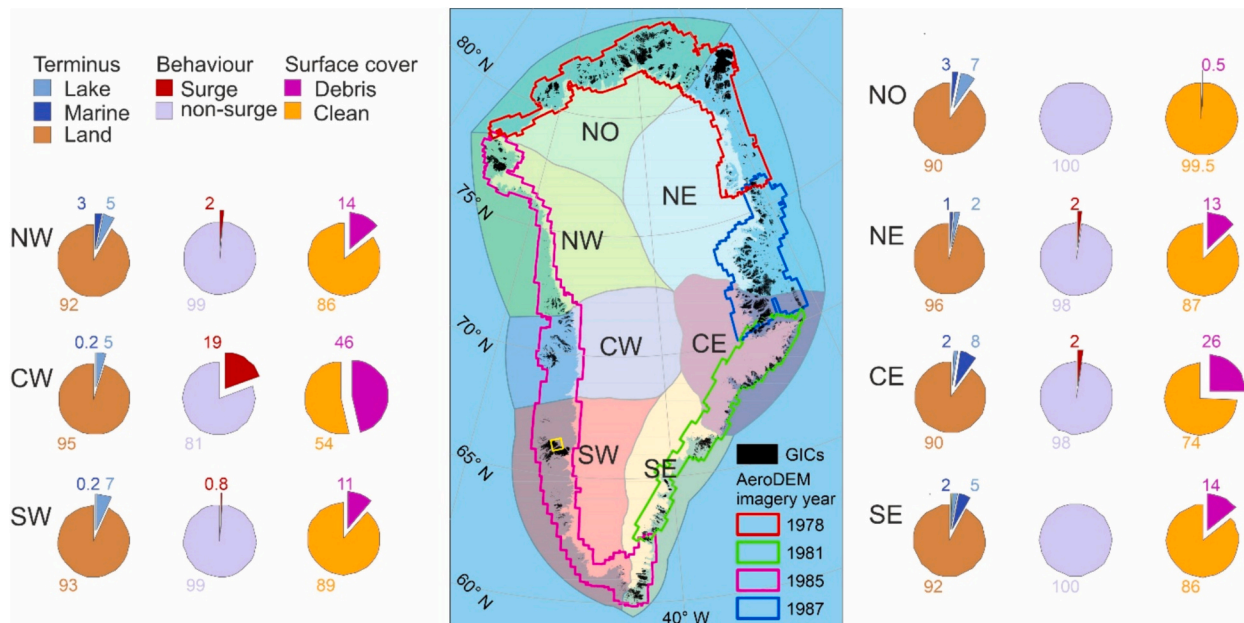

Fig. 1. Location of peripheral glaciers and ice caps across Greenland and AeroDEM data coverage by year. Pie charts indicate percentage of glaciers within each region categorised by terminus, behaviour and surface type. Yellow extent box in south west Greenland shows location of Fig. 2. (For interpretation of the references to colour in this figure legend, the reader is referred to the web version of this article.)

analysis, and any glaciers with a 'form' attribute value of 2 'perennial snowfield' or 3 'seasonal snowfield' were also excluded from our analysis.

2.3. Glacier ablation area delineation

The low-contrast of snow-covered higher-elevation parts of the landscape necessitated widespread interpolation for the AeroDEM. For glaciers, this means that accumulation areas frequently contain large artefacts in the AeroDEM and steep elevation irregularities are common. However, the distinct contrast between bare ice, snow and surrounding ice free areas means that lower-elevation parts; glacier ablation areas, are well-resolved and largely free of these artefacts. Therefore, in this study we only analysed elevation changes within glacier ablation areas.

Ablation areas were defined by intersecting a glacier-specific equilibrium line altitude (ELA) with a glacier outline. Glacier-specific ELAs were defined using an automated Area Altitude Balance Ratio tool (Pellitero et al., 2015) as modified and developed to produce ablation areas automatically for thousands of glaciers in several world regions (Carrivick et al., 2019, 2020a, 2022a, 2022b, 2023; Lee et al., 2021). In this study we used a balance ratio of 2.24 as suggested to be representative for high latitude glaciers (Rea, 2009) but we note that value is based only a very small sample of glaciers. The few Greenland GICs with direct measurements of mass balance (Machguth et al., 2016) have a wide range of BR values, but our sensitivity testing shows that our mass balance estimates are only weakly sensitive to our choice of BR value (Table SI.1). Nonetheless, acknowledging this uncertainty in glacier-specific ELAs, we only report our results for large spatial aggregations of glaciers rather than for individual GICs.

2.4. Elevation change grids

We used the reliability mask of the AeroDEM to mitigate artefacts remaining within ablation areas. Although Korsgaard et al. (2016) recommend retaining areas with reliability values $\geq$ 40, that recommendation was based on calculations across the whole landscape(s) and the worst areas of the AeroDEM vertical accuracy relate to poor photogrammetric elevation extraction over steep terrain (shadow effects) and glacier accumulation areas (poor contrast across snow effects). Our interrogation of the AeroDEM reliability mask within GIC ablation areas showed reliability values only between 22 and 39 and therefore we retained cells with reliability values >22. Glaciers north of 82.6^o N and on small east coast islands were removed from our analysis due to the poor quality of the GIMP DEM in these regions, caused by the poor quality of Landsat imagery above this latitude.

Elevation change gridswere filtered to only retain those cells within 3 standard deviations of the local (per ablation area) mean. That filter preserved 99.7% of data per AeroDEM timescale region and using an empirical three-sigma rule is similar to the filtering applied by Huber et al. (2020). This process was iterated until the mean and standard deviation of the elevation change grids were below 0.01 m, usually on the fourth iteration.

2.5. Void filling

Voids in the elevation change grids introduced by the reliability masking and recursive three-sigma rule filtering were filled using interpolation (c.f. Huber et al., 2020, Seehaus et al., 2020, McNabb et al., 2017, 2019b). Specifically, a two-part approach (c.f. von Albedyll et al., 2018; Magnússon et al., 2016) was applied. Firstly, small single-pixel voids were replaced by calculating the average of surrounding cells (in eight directions) and applying a plane-fitting algorithm. For larger voids >1 pixel an inverse distance weighted algorithm was applied. Just <3% of ablation areas whose voids exceeded 50% of the total ablation area were completely removed from analysis.

2.6. Final filtering and groupings of glaciers

Of the total 17,334 Greenland GICs (RGI v6.0) we excluded all those <1 km^2 due to their ablation areas having an average area less than three cells (0.0027 km^2) in area. This final filter reduced the number of glaciers to 6149 or < 36%, with the total glacier area reduced to 83,312 km^2 but retaining >96% and 99% of the whole glacier, or of ablation areas, respectively.

We also mitigated any localised DEM errors and hence glacier-specific uncertainties by aggregating our results onto a 500 km^2 tessellation grid Greenland-wide, by region and by glacier type. Following Lee et al. (2021) we consider six mutually-exclusive groupings of glacier type by terminus (lake, marine, and land) and surface (clean and debris), which for Greenland GICs are: i) lake-clean ($n = 169$, 2.7%), ii) lake-debris ($n = 61$, 1%), iii) marine-clean ($n = 153$, 2.5%), iv) marine-debris ($n = 42$, 0.7%), v) land-clean ($n = 4761$, 77.4%), and vi) land-debris (963, 15.7%) (Fig. 1). Debris cover was taken from Herreid and Pellicciotti (2020), terminus type was determined from intersecting glacier outlines with lakes and the coastline and surge status was determined from Lovell et al. (2023).

2.7. Conversion of elevation change grids to volume and calculation of mass and mass balance

Void-filled elevation change grids were converted to volume change (ΔV, m^3) by summing all elevation change cells (Δh, m^2) and multiplying by the cell size for each glacier ablation area. Volume change was converted to mass change (kg^3) using an ice density of 850 kg m^{-3} (Huss, 2013).

In order to mitigate erroneous and ultra-low confidence data that is widespread within glacier accumulation areas, to compare our datasets that span different times, and to enable comparison with other published studies, we estimate glacier mass balance by assuming no volume change above the ELA; i.e. by dividing our volume change in ablation areas by glacier area. This mass balance estimate is not necessarily a minimum because if for a given glacier the accumulation area were to be included and thus slightly more volume loss was computed that would be off-set by the much larger glacier extent (including accumulation area). Therefore, we compare our results of the time period 1978 to 2015 to the more recent annual rates of change reported by Hugonnet et al. (2021) by clipping their *dh/dt* grids to our ablation areas.

2.8. Error and uncertainty

Analysing geodetic changes only within glacier ablation areas via the use of an automated AABR tool enables us to make Greenland-wide inter-regional comparisons with large numbers of glaciers. However, this approach does also mean that for individual glaciers some small parts of an accumulation area (in addition to the ablation area) could be included, whilst for other glaciers the full ablation area might not be included in our elevation change analysis (Fig. SI.1). These under- and over-estimations will cancel out as we aggregate our results for large groups of glaciers only. Additionally, whilst down-wasting probably dominates the mass loss geometric signal over terminus recession, it can be expected that glaciers have become smaller during our study period, and so using a fixed (RGI_v6 outline) geometry for our elevation change analysis will probably slightly underestimate mass loss. Therefore, we present our results as the median of large groups of glaciers. Therefore the spatial patterns and temporal trends that we identify are robust, whilst our quantification of mass balance is most likely a minimum estimate.

Random and systematic error and uncertainty in our calculated elevation changes are introduced in three forms: i) error within the static DEMs introduced during acquisition (i.e. shadow, clouds, sensor instability, poor ground illumination conditions) and preparation (georeferencing inaccuracy and pre-processing such as void filling and

interpolation); ii) processing errors introduced by imperfect alignment during co-registration and resampling from native to lower resolutions; and iii) temporal uncertainty due to imprecise dates; the GIMP and ArcticDEM DEMs and mosaics of images collected over a time span. We calculated the random and systematic uncertainty in our surface elevation measurement with the Normalized Median Absolute Deviation (NMAD), standard deviation, and mean of elevation changes over off-ice surfaces considered to be static over the study period (Table SI.2). Whilst the GIMP DEM is the poorest quality dataset (Table SI.2), it was also constructed from images gathered across an unspecified time span, and so those attributes produce a relatively very high uncertainty when using it in calculations of rates of change and so we exclude it from our mass balance calculations.

To quantify the overall uncertainty associated with our mass balance calculations $\sigma_{\Delta M}$ we account for these random and systematic errors in our elevation change measurements $\sigma_{\Delta h}$ and combine these with temporal uncertainty $\sigma_{\Delta t}$ (from imprecise DEM acquisition dates), area uncertainty σ_A (from inaccuracies in the glacier outlines), and the density uncertainty σ_ρ associated with the constant standard bulk density estimate used of 850 kg m^{-3}. We combine these four uncertainty metrics ($\sigma_{\Delta h}$, $\sigma_{\Delta t}$, σ_A, and σ_ρ) into our mass balance formula as calculated per difference DEM to then calculate per glacier and regional mass balance uncertainty. We outline our full uncertainty assessment with equations in Supplementary Information.

3. Results

3.1. Glacier volume and mass change

Our *dH/dt* grids (Fig. 2) reveal that Greenland GICs lost at least 276 ± 55 Gt of ice, or 0.76 ± 0.15 mm sea level rise equivalent between the late 1970s and 2015. Overall, all regions of Greenland had negative mass balance and the Greenland-wide GIC median mass balance from 1978 to 2015 was −0.1 ± 0.02 m w.e. yr^{-1}. GICs on the west of Greenland have experienced more negative mass balances than those on the east (Fig. 3).

Median mass balance is more negative on both coasts at lower latitudes, with north Greenland having the least negative mass balance (−0.05 ± 0.02 m w.e. yr^{-1}), followed by the north east (−0.08 ± 0.02 m w.e. yr^{-1}), central east (−0.08 ± 0.02 m w.e. yr^{-1}) and south east (−0.13 ± 0.03 m w.e. yr^{-1}). The south east is the only region in the east where the GIC mass balance (−0.10 ± 0.02 m w.e. yr^{-1}) is less than the Greenland wide average rate. Post-hoc Wilcoxon test results show that all regions have statistically significant differences in mass balance except the adjacent north and central east areas.

Mindful of the high uncertainties associated with our sub-periods due to the GIMP DEM, we show that mass loss has accelerated across Greenland between the 1980s and 2010s except within the south and
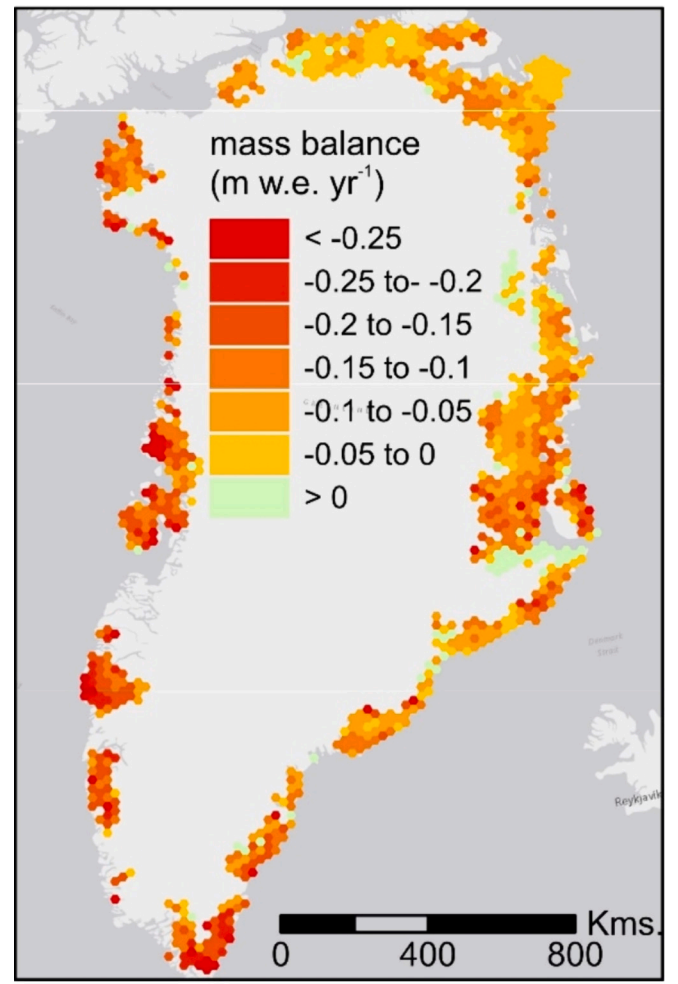

Fig. 3. Greenland-wide pattern of GIC mass balance varying from 1978 to 87 to 2015 displayed using the median mass balance of tens of glaciers within each 500 km^2 tessellation cell. Exact dates and hence duration vary spatially as illustrated in Fig. 1.

central east regions (Figs. SI·2B, SI2C). West Greenland GICs had the most negative mass balance, and experienced a 2.7 times increase in mass loss (from −0.10 to −0.27 m w.e. yr^{-1}) in the SW and a 5.6 times increase (from 0.06 to 0.34 m w.e. yr^{-1}) in the CW (Figs. SI·2B, SI2C). There was a negligible effect of whether or not we included surge-type glaciers in our regional volume and mass balance calculations
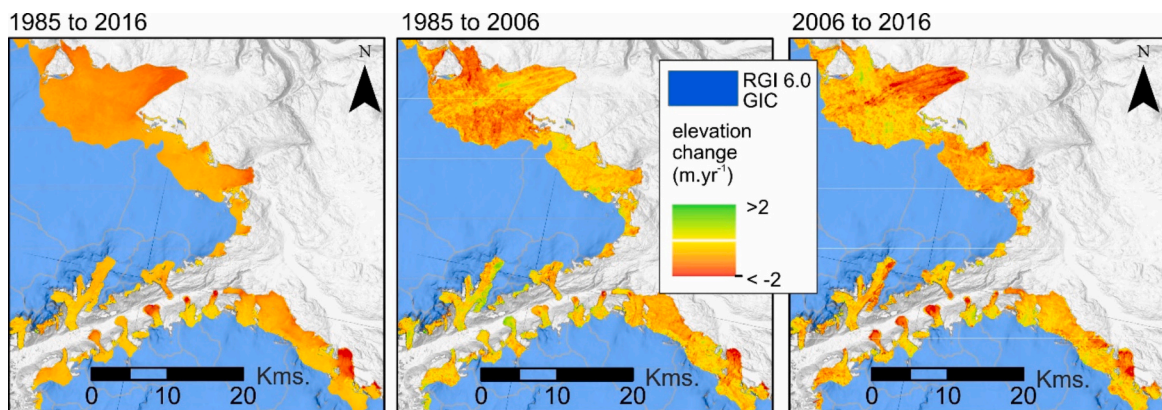

Fig. 2. Example of accelerated surface elevation changes for outlet glacier on the north east of the Maniitsoq ice cap, south west Greenland (shown by yellow extent box in Fig. 1). (For interpretation of the references to colour in this figure legend, the reader is referred to the web version of this article.)

(Table SI.3).

3.2. Variations by glacier terminus environment, behaviour and surface character

Median mass balance from 1978 to 2015 varied by glacier terminus type and surface character, in order from most negative as: lake-debris (-0.15 ± 0.02 m w.e. yr^{-1}), marine-debris (-0.13 ± 0.02 m w.e. yr^{-1}), lake-clean (-0.12 ± 0.02 m w.e. yr^{-1}), land-debris (-0.11 ± 0.02 m w.e. yr^{-1}), land-clean (-0.09 ± 0.02 m w.e. yr^{-1}), and marine-clean (0.08 ± 0.02 m w.e. yr^{-1}) (Fig. 4). Debris covered Greenland GICs tend to have a more negative mass balance than clean surface glaciers (Fig. 4). Water-terminating Greenland GICs tend to have a more negative mass balance than land terminating glaciers (Fig. 4). Glaciers terminating in lakes have the most negative mass balances, more-so than those terminating in oceans (Fig. 4). Water-terminating glaciers across Greenland also have more variation (a higher inter-quartile range) in their mass balance than land-terminating glaciers (Fig. 4).

The groups with the most negative mass balances (where $n > 4$) are found in the south east region with three of these groups being water-terminating and the lowest being debris covered: lake-debris (-0.28 ± 0.03 m w.e. yr^{-1}), marine-debris (-0.25 ± 0.03 m w.e. yr^{-1}), land-debris (-0.23 ± 0.03 m w.e. yr^{-1}), and lake-clean (-0.21 ± 0.03 m w.e. yr^{-1}). The fifth lowest mass balance of any group is for clean lake-terminating glaciers in south west Greenland (-0.21 ± 0.03 m w.e. yr^{-1}). Taken together, these results evidence that mass balance of Greenland GICs is controlled by the compounding influences of latitude, terminus environment and glacier surface character.

4. Discussion

4.1. Mass balance and glacier type

Lake-terminating glaciers have been found to have enhanced terminus recession, ice surface velocity and to more negative mass balance than their land-terminating counterparts in several ice sheet and alpine settings (King et al., 2018, 2019; Pronk et al., 2021; Mallalieu et al., 2021) owing to a series of thermo-mechanical feedbacks and

interactions between lakes and glaciers (Carrivick et al., 2020a, 2020b; Sutherland et al., 2020). The time-scale over which these lake effects on glaciers persist depends on local topography; the shape and size of the lake, as well as ice dynamics.

Marine-terminating glaciers have multiple forcings that expedite calving and mass loss in excess of climate forcing alone (Van As et al., 2014; Rignot et al., 2015; McMillan et al., 2016). However, we find that marine-terminating glaciers have amongst the least negative mass balance of our glacier type groupings (Fig. 4). We consider that this unexpected finding can be explained by the location of the GICs; 84% of marine-terminating glaciers are in eastern Greenland where evidence of increasing glacier mass has been reported Hugonnet et al., 2021; Sørensen et al., 2018), and acceleration of mass loss has occurred since 1999 to 2018 (Bollen et al., 2023).

Many glaciers worldwide accrue thick insulating debris cover sourced from rockfall from steep valley sides and that thick debris insulates underlying ice from melt. However, debris cover on Greenland GICs is more limited in extent being just 2.4% of total glacier area (Scherler et al., 2018). Furthermore, we suggest based on satellite images that debris on Greenland GIC is mostly composed of relatively thin veneers of aeolian-derived material, cryoconite (Takeuchi et al., 2018), ogive-bands, surficial glaciofluvial sediment, and melt out till (Yde and Knudsen, 2005), due to a lack of steep valley sides to supply coarse rockfall material in many areas or due to exceptionally hard bedrock in others. Such thin debris cover lowers surface albedo and thus explains the enhanced mass loss that we find on debris-covered Greenland GICs (Fig. 4). We acknowledge that the debris cover on some glaciers could have changed during our study period, and that the properties of supraglacial debris on Greenland GICs are almost unknown, whereas a few studies have detailed the surface composition of parts of the GrIS (Bøggild et al., 2010; Ryan et al., 2018).

Whilst surge-type glaciers might be expected to have a gain of mass in ablation areas, we find in this study that surge-type glaciers are associated with more negative mass balance than non-surge type glaciers. This finding perhaps indicates that these glaciers surged prior to the first time period of this study (late 1970s to 2006) and therefore have since experienced rapid mass loss in their ablation zones (Truffer et al., 2021). For example, of 63 glaciers identified as surge type in central
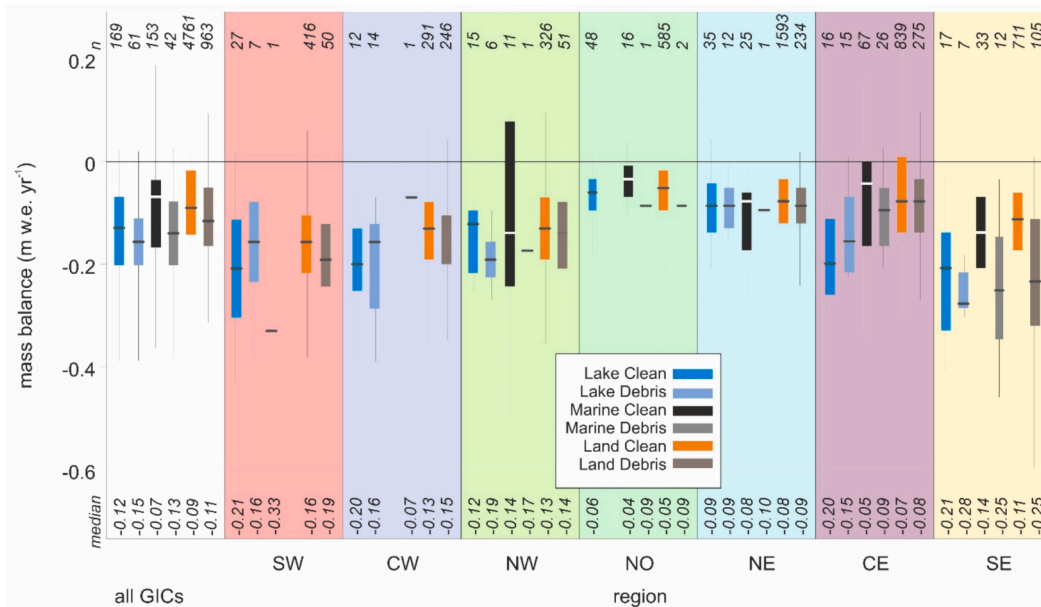

Fig. 4. Variation of mass balance with terminus type and surface character. Counts (*n*) of glacier type per region are shown along the top of the chart, and median mass balance values at the bottom. Note that some regions do not contain any glaciers in these categories and some categories contain too few glaciers to calculate an inter-quartile ranges.

western Greenland, only 11 exhibited a surge-type elevation profile change between 1985 and 2012 (Huber et al., 2020). The reverse pattern in the south-west region suggests that these surges occurred more recently.

4.2. Comparison with contemporary mass balance around Greenland

Our *GIC* mass balance for 1978 to 2015 is slightly less negative than the longer-term rate calculated since the Little Ice Age (LIA) by Carrivick et al. (2023), and less negative within all regions than for rates calculated since the year 2000 (Hugonnet et al., 2021) (Fig. 5). There has therefore been a net acceleration of mass loss from Greenland GICs not only since the LIA but most especially since the late 1970s and before 2000 (Table 1, Fig. 5). The most recent rate of Greenland-wide mass loss (2015 to 2019) seems to be approaching the longer-term mean since the LIA (Fig. 5), which suggests that mass loss must have been much less negative, perhaps even positive mass balance for GICs in the 1980s and 1990s (Figs. 3, 4, 5), which is plausible given that the GrIS was more or less in state of balance during the 1970s (Rignot et al., 2008) and during the 1990s (Shepherd et al., 2020). However, there is considerable variability in mass loss rates through time across Greenland; GIC mass balance has become progressively less negative in the south east, central east, and north east regions since the year 2000, whereas since the 1980s it has become progressively more negative in the western regions (Fig. 5).

Our findings of an east-west asynchrony across Greenland in GIC mass loss support those of other remote-sensing-based studies but we consider a longer time-frame and reveal greater complexity by region and by glacier type than before. The few direct field measurements of glacier mass balance also show differences between glaciers on the west and east of Greenland (Machguth et al., 2016). These glacier responses are linked to temperature-precipitation trends, which are often opposite between west and east Greenland (Box, 2002). Bjørk et al. (2018) suggest that the west-east disparity could become more marked with North Atlantic Oscillation (NAO) becomes more positive with ongoing climate change.

It is also apparent that glacier mass balance is generally less negative when longer time periods of study are considered (Table 1). For example, our 37-year study period has a net geodetic mass balance of 0.3 m w.e yr^{-1} for ablation areas, which is less negative than the mass balance calculated from studies focussing on shorter and more recent

Table 1

Comparison of GIC mass balance across Greenland by time period, calculated from mass losses reported by a number of modelling, geodetic and gravimetric studies (and accommodating different glacier areas analysed between studies).

Time period	Duration (years)	Mass Balance (m w.e. yr^{-1})	Method	Study
1900 to 2015	115	−0.06 ± 0.02	modelled	Carrivick et al. (2023)
1958 to 1996	39	−0.14 ± 0.19	modelled	Noël et al. (2017)
1978 to 2016	37	−0.30 ± 0.02	geodetic	This study ablation areas
2003 to 2008	5	−0.31 ± 0.13	geodetic	Bolch et al. (2013)
2003 to 2009	6	−0.43 ± 0.13	gravimetric	Colgan et al. (2015)
2000 to 2020	20	−0.40 ± 0.07	geodetic	Hugonnet et al. (2021)
2003 to 2009	6	−0.42 ± 0.08	geodetic	Gardner et al. (2013)
1997 to 2015	18	−0.44 ± 0.19	modelled	Noël et al. (2017)
1985 to 2012	27	−0.45 ± 1.59	geodetic	Huber et al. (2020) (*extrapolated)
2006 to 2016	10	−0.63 ± 0.21	geodetic	Zemp et al. (2019)

time periods (Table 1). The least negative rate is that reported by Noël et al. (2017); −0.14 m w.e. yr^{-1} for the 39 year time period 1958 to 1997. Contrastingly, they report −0.44 m w.e. yr^{-1} for the 18 year time period of 1997 to 2015, which is almost as negative as the extrapolation of Huber et al. (2020) and the geodetic calculation of Zemp et al., 2019 for the 10 year time period 2006 to 2016 (Table 1).

Our results should assist with refinement of global glacier evolution models (Marzeion et al., 2012; Huss and Hock, 2015; Rounce et al., 2023), which rely on calibration during a baseline time period before projecting into the future. The Greenland population of glaciers pose problems for numerical models due to data gaps and relatively wide-spread model failure (e.g. 20% of total glacier surface area; c.f. table 2 of Marzeion et al., 2012) leading to likely bias, or systematic error and hence relatively high uncertainty in model results across this region Marzeion et al., 2020).
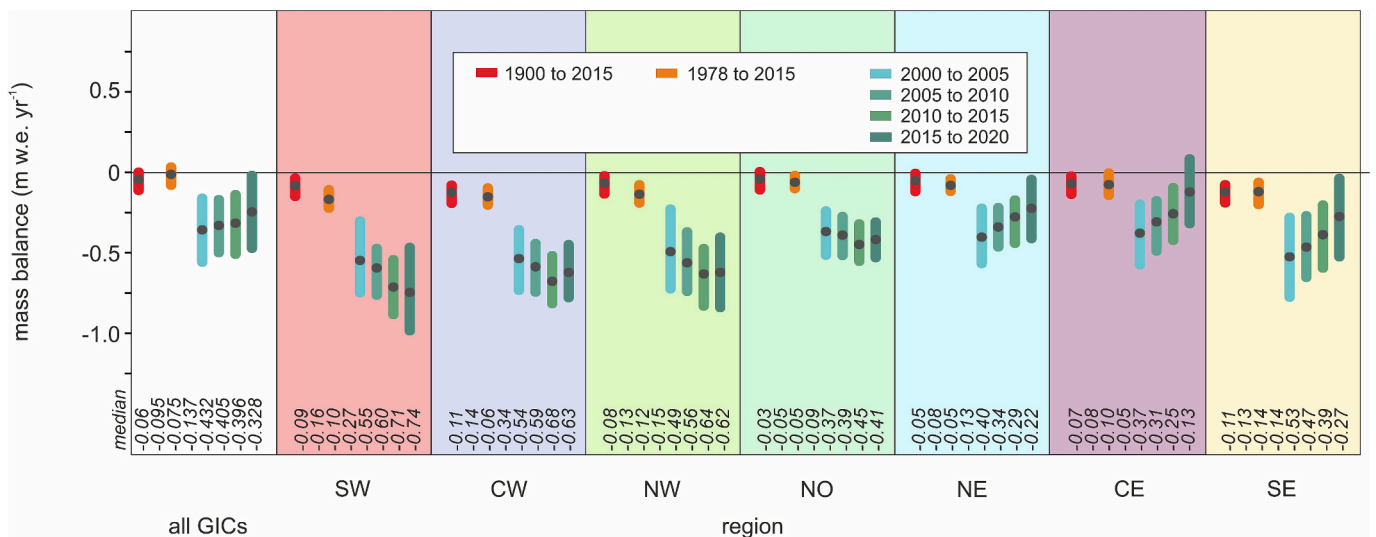

Fig. 5. Comparison between our estimates of GIC mass balance between 1878 and 2015 and Greenland-wide and per region rates that have been reconstructed for since the Little Ice Age termination (year 1900) by Carrivick et al. (2023) and for four time periods since 2000 by Hugonnet et al. (2021). The dots represent median values, and the coloured bars represent the uncertainty range.

4.3. Summary and conclusions

We present the first Greenland-wide surface elevation changes of GICs at 30 m resolution from the late 1970s and 2015. We include all 6149 glaciers larger than 1 km^2, accounting for >96% of Greenland GICs and 99% of all GIC area. Our analysis is restricted to glacier ablation areas, which enables us to maintain high accuracy in our elevation change datasets, but necessitates us to assume no mass loss above the altitude of our estimated equilibrium lines.

Overall, we find that Greenland GICs have experienced mass loss in their ablation areas of at least -8.5 ± 1.53 Gt yr^{-1}, equating to -0.0003 Gt yr^{-1} per km^2 for the time period 1978 to 2015. Putting together our 1978 to 2015 GIC mass balance, our analysis of Hugonnet et al.'s (2021) dataset for Greenland, comparison to Carrivick et al.'s (2023) long-term mass balance since the LIA, and GIC mass balance over recent decades from the literature (Table 1) in combination evidence an acceleration in mass loss from Greenland GICs during the late 20th/early 21st century. However, these Greenland-wide values hide considerable spatio-temporal heterogeneity.

We quantify that glacier mass balance rates were most negative in southern Greenland and less negative towards the north up to 2015. However, the results of Khan et al., 2022 show increasingly negative mass balance in the north up to 2021. We find that some glaciers in some regions experienced positive mass balances (Fig. 4). Glaciers in west Greenland have had significantly more negative mass balances since the late 1970s than those in the east. Furthermore, glaciers in east Greenland have had a decelerating mass loss since the year 2000 whereas the mass loss of western glaciers has continued to accelerate since the 1980s. Therefore, the Greenland-wide signal of mass loss up to 2015 was dominated by glaciers in the east (Fig. 4).

Lake-terminating glaciers and those with debris cover have experienced the most negative mass balance rates compared to those that are marine- or land-terminating and to those with clean ice surfaces. These controls of glacier type on mass loss suggest that glacier evolution models should consider incorporating terminus environment and surface characteristics to refine projections of mass loss and sea level contributions.

Our quantification of the spatially heterogeneous rates of mass loss across Greenland should be useful for understanding climate change across the region, given that GICs are relatively sensitive to climate change (in comparison to the GrIS), and given that weather station records and river runoff records across Greenland are extremely sparsely distributed and do not tend to extend back more than a few decades at most. Glacier mass loss and consequent meltwater production has implications for proglacial fluvial dynamics, hydrological connectivity and hence for freshwater, sediment/mineral and nutrient export to the oceans. On a local scale, these factors affect indigenous communities' sustainability, economically-important salmon behaviour, and economically-important hydropower and sand mining, for example. More widely, meltwater from Greenland GICs will produce freshening of arctic oceans that could have complex implications for coastal biodiversity, and they will remain an important contribution to global sea level rise.

Author contributions

MG conceived the study and with JLC and MWS designed the analysis. MG conducted all the data acquisition, pre-processing and all the analysis, and led the manuscript writing. All authors contributed to writing the manuscript.

CRediT authorship contribution statement

Michael Grimes: Writing – review & editing, Writing – original draft, Methodology, Formal analysis, Conceptualization. **Jonathan L. Carrivick:** Writing – review & editing, Supervision. **Mark W. Smith:** Writing – review & editing, Supervision.

Declaration of competing interest

The authors declare that they have no known competing financial interests or personal relationships that could have appeared to influence the work reported in this paper.

Data availability

Our dH grid datasets are available from the NERC CEDA data repository at https://catalogue.ceda.ac.uk/uuid/85c7d97c5d104a329 89b13abc3f8ea5d.

Appendix A. Supplementary data

Supplementary data to this article can be found online at https://doi.org/10.1016/j.gloplacha.2024.104505.

References

Beyer, R.A., Alexandrov, O., McMichael, S., 2018. The Ames Stereo Pipeline: NASA's open source software for deriving and processing terrain data. Earth Space Sci. 5 (9), 537–548.

Bintanja, R., Selten, F.M., 2014. Future increases in Arctic precipitation linked to local evaporation and sea-ice retreat. Nature 509 (7501), 479.

Bjørk, A.A., Kjær, K.H., Korsgaard, N.J., Khan, S.A., Kjeldsen, K.K., Andresen, C.S., Box, J. E., Larsen, N.K., Funder, S., 2012. An aerial view of 80 years of climate-related glacier fluctuations in southeast Green-land. Nat. Geosci. 5 (6), 427–432.

Bjørk, A.A., Aagaard, S., Lütt, A., Khan, S.A., Box, J.E., Kjeldsen, K.K., Larsen, N.K., Korsgaard, N.J., Cappelen, J., Colgan, W.T., Machguth, H., Andresen, C.S., Peings, Y., Kjær, K.H., 2018. Changes in Greenland's peripheral glaciers linked to the North Atlantic Oscillation. Nat. Clim. Chang. 8 (1), 48–52.

Bøggild, C.E., Brandt, R.E., Brown, K.J., Warren, S.G., 2010. The ablation zone in Northeast Greenland: ice types, albedos and impurities. J. Glaciol. 56 (195), 101–113.

Bolch, T., Sorensen, L.S., Simonsen, S.B., Molg, N., Machguth, H., Rastner, P., Paul, F., 2013. Mass loss of Greenland's glaciers and ice caps 2003-2008 revealed from ICESat laser altimetry data. Geophys. Res. Lett. 40 (5), 875–881.

Bollen, K.E., Enderlin, E.M., Muhlheim, R., 2023. Dynamic mass loss from Greenland's marine-terminating peripheral glaciers (1985–2018). J. Glaciol. 69 (273), 153–163.

Box, J.E., 2002. Survey of Greenland instrumental temperature records: 1873-2001. Int. J. Climatol. 22 (15).

Candela, S.G., Howat, I., Noh, M.-J., Porter, C.C., Morin, P.J., 2017. ArcticDEM validation and accuracy assessment. In: AGU Fall Meeting Abstracts pp.C51A-0951.

Carrivick, J.L., Boston, C.M., King, O., James, W.H.M., Quincey, D.J., Smith, M.W., Grimes, M., Evans, J., 2019. Accelerated volume loss in Glacier Ablation zones of NE Greenland, Little Ice Age to present. Geophys. Res. Lett. 46 (3), 1476–1484.

Carrivick, J.L., James, W.H., Grimes, M., Sutherland, J.L., Lorrey, A.M., 2020a. Ice thickness and volume changes across the Southern Alps, New Zealand, from the little ice age to present. Sci. Rep. 10 (1), 13392.

Carrivick, J.L., Tweed, F.S., Sutherland, J.L., Mallalieu, J., 2020b. Toward numerical modeling of interactions between ice-marginal proglacial lakes and glaciers. Frontiers. Earth Sci. 500.

Carrivick, J.L., How, P., Lea, J.M., Sutherland, J.L., Grimes, M., Tweed, F.S., Cornford, S., Quincey, D.J., Mallalieu, J., 2022a. Ice-marginal proglacial lakes across Greenland: present status and a possible future. Geophys. Res. Lett. 49 (12), e2022GL099276.

Carrivick, J.L., Sutherland, J.L., Huss, M., Purdie, H., Stringer, C.D., Grimes, M., James, W.H., Lorrey, A.M., 2022b. Coincident evolution of glaciers and ice-marginal proglacial lakes across the Southern Alps, New Zealand: past, present and future. Glob. Planet. Chang. 211, 103792.

Carrivick, J.L., Boston, C.M., Sutherland, J.L., Pearce, D., Armstrong, H., Bjørk, A., Kjeldsen, K.K., Abermann, J., Oien, R.P., Grimes, M., 2023. Mass loss of glaciers and ice caps across Greenland since the Little Ice Age. Geophys. Res. Lett. 50 (10), e2023GL103950.

Chylek, P., Folland, C.K., Lesins, G., Dubey, M.K., Wang, M.Y., 2009. Arctic air temperature change amplification and the Atlantic Multidecadal Oscillation. Geophys. Res. Lett. 36 (14).

Colgan, W., Abdalati, W., Citterio, M., Csatho, B., Fettweis, X., Luthcke, S., Moholdt, G., Simonsen, S.B., Stober, M., 2015. Hybrid glacier Inventory, Gravimetry and Altimetry (HIGA) mass balance product for Greenland and the Canadian Arctic. Remote Sens. Environ. 168, 24–39.

Fettweis, X., Hanna, E., Gallee, H., Huybrechts, P., Erpicum, M., 2008. Estimation of the Greenland ice sheet surface mass balance for the 20th and 21st centuries. Cryosphere 2 (2), 117–129.

Fettweis, X., Franco, B., Tedesco, M., van Angelen, J.H., Lenaerts, J.T.M., van den Broeke, M.R., Gallee, H., 2013. Estimating the Greenland ice sheet surface mass balance contribution to future sea level rise using the regional atmospheric climate model MAR. Cryosphere 7 (2), 469–489.

Gardner, A.S., Moholdt, G., Cogley, J.G., Wouters, B., Arendt, A.A., Wahr, J., Berthier, E., Hock, R., Pfeffer, W.T., Kaser, G., Ligtenberg, S.R.M., Bolch, T., Sharp, M.J., Hagen, J.O., van den Broeke, M.R., Paul, F., 2013. A reconciled estimate of glacier contributions to sea level rise: 2003 to 2009. Science 340 (6134), 852–857.

Goelzer, H., Huybrechts, P., Furst, J.J., Nick, F.M., Andersen, M.L., Edwards, T.L., Fettweis, X., Payne, A.J., Shannon, S., 2013. Sensitivity of Greenland ice sheet projections to model formulations. J. Glaciol. 59 (216), 733–749.

Hanna, E., Cappelen, J., Fettweis, X., Mernild, S.H., Mote, T.L., Mottram, R., Steffen, K., Ballinger, T.J., Hall, R.J., 2021. Greenland surface air temperature changes from 1981 to 2019 and implications for ice-sheet melt and mass-balance change. Int. J. Climatol. 41, E1336–E1352.

Herreid, S., Pellicciotti, F., 2020. The state of rock debris covering Earth's glaciers. Nat. Geosci. 13 (9), 621–627.

Holland, M.M., Bitz, C.M., 2003. Polar amplification of climate change in coupled models. Clim. Dyn. 21 (3–4), 221–232.

Hopwood, M.J., Carroll, D., Dunse, T., Hodson, A., Holding, J.M., Iriarte, J.L., Ribeiro, S., Achterberg, E.P., Cantoni, C., Carlson, D.F., 2020. How does glacier discharge affect marine biogeochemistry and primary production in the Arctic? Cryosphere 14 (4), 1347–1383.

Howat, I.M., Negrete, A., Smith, B.E., 2014. The Greenland Ice Mapping Project (GIMP) land classification and surface elevation data sets. Cryosphere 8 (4), 1509–1518.

Howat, I., Negrete, A., Smith, B., 2015. MEaSUREs Greenland ice mapping project (GIMP) digital elevation model, version 1. Cryosphere 8, 1509–1518.

Huber, J., McNabb, R., Zemp, M., 2020. Elevation changes of west-Central Greenland glaciers from 1985 to 2012 from remote sensing. Front. Earth Sci. 8, 35.

Hugonnet, R., McNabb, R., Berthier, E., Menounos, B., Nuth, C., Girod, L., Farinotti, D., Huss, M., Dussaillant, I., Brun, F., Kääb, A., 2021. Accelerated global glacier mass loss in the early twenty-first century. Nature 592 (7856).

Huss, M., 2013. Density assumptions for converting geodetic glacier volume change to mass change. Cryosphere 7 (3), 877–887.

Huss, M., Hock, R., 2015. A new model for global glacier change and sea-level rise. Front. Earth Sci. 3, 54.

Khan, S.A., Colgan, W., Neumann, T.A., Van Den Broeke, M.R., Brunt, K.M., Noël, B., Bamber, J.L., Hassan, J., Bjørk, A.A., 2022. Accelerating ice loss from peripheral glaciers in North Greenland. Geophys. Res. Lett. 49 (12) p.e2022GL098915.

King, O., Dehecq, A., Quincey, D., Carrivick, J., 2018. Contrasting geometric and dynamic evolution of lake and land-terminating glaciers in the central Himalaya. Glob. Planet. Chang. 167, 46–60.

King, O., Bhattacharya, A., Bhambri, R., Bolch, T., 2019. Glacial lakes exacerbate Himalayan glacier mass loss. Sci. Rep. 9 (1), 18145.

Knox, J.C., 1993. Large increases in Flood Magnitude in Response to modest changes in climate. Nature 361 (6411), 430–432.

Korsgaard, N.J., Nuth, C., Khan, S.A., Kjeldsen, K.K., Bjork, A.A., Schomacker, A., Kjaer, K.H., 2016. Digital elevation model and orthophotographs of Greenland based on aerial photographs from 1978-1987. Sci. Data. 3, 160032.

Krisch, S., Browning, T.J., Graeve, M., Ludwichowski, K.U., Lodeiro, P., Hopwood, M.J., Roig, S., Yong, J.C., Kanzow, T., Achterberg, E.P., 2020. The influence of Arctic Fe and Atlantic fixed N on summertime primary production in Fram Strait, North Greenland Sea. Sci. Rep. 10 (1).

Lee, E., Carrivick, J.L., Quincey, D.J., Cook, S.J., James, W.H.M., Brown, L.E., 2021. Accelerated mass loss of Himalayan glaciers since the Little Ice Age. Sci. Rep. 11 (1), 24284.

Lovell, H., Carrivick, J.L., King, O., et al., 2023. Surge-type glaciers in Kalaallit Nunaat (Greenland): distribution, temporal patterns and climatic controls. J. Glaciol. 1–18. https://doi.org/10.1017/jog.2023.61. Published online.

Machguth, H., Rastner, P., Bolch, T., Molg, N., Sorensen, L.S., Aoalgeirsdottir, G., van Angelen, J.H., van den Broeke, M.R., Fettweis, X., 2013. The future sea-level rise contribution of Greenland's glaciers and ice caps. Environ. Res. Lett. 8 (2).

Machguth, H., Thomsen, H.H., Weidick, A., Ahlstrøm, A.P., Abermann, J., Andersen, M.L., Andersen, S.B., Bjørk, A.A., Box, J.E., Braithwaite, R.J., 2016. Greenland surface mass-balance observations from the ice-sheet ablation area and local glaciers. J. Glaciol. 62 (235), 861–887.

Magnússon, E., Muñoz-Cobo Belart, J., Pálsson, F., Ágústsson, H., Crochet, P., 2016. Geodetic mass bal-ance record with rigorous uncertainty estimates deduced from aerial photographs and lidar data–Case study from Drangajökull ice cap, NW Iceland. Cryosphere 10 (1), 159–177.

Mallalieu, J., Carrivick, J.L., Quincey, D.J., Raby, C.L., 2021. Ice-marginal lakes associated with enhanced recession of the Greenland Ice Sheet. Glob. Planet. Chang. 202, 103503.

Marzeion, B., Jarosch, A.H., Hofer, M., 2012. Past and future sea-level change from the surface mass balance of glaciers. Cryosphere 6 (6), 1295–1322.

Marzeion, B., Hock, R., Anderson, B., Bliss, A., Champollion, N., Fujita, K., Huss, M., Immerzeel, W.W., Kraaijenbrink, P., Malles, J.H., Maussion, F., 2020. Partitioning the uncertainty of ensemble projections of global glacier mass change. Earth's Future 8 (7) p.e2019EF001470.

Mayewski, P.A., Sneed, S.B., Birkel, S.D., Kurbatov, A.V., Maasch, K.A., 2014. Holocene warming marked by abrupt onset of longer summers and reduced storm frequency around Greenland. J. Quat. Sci. 29 (1), 99–104.

McMillan, M., Leeson, A., Shepherd, A., Briggs, K., Armitage, T.W.K., Hogg, A., Kuipers Munneke, P., Van Den Broeke, M., Noël, B., van de Berg, W.J., 2016. A high-resolution record of Greenland mass balance. Geophys. Res. Lett. 43 (13), 7002–7010.

McNabb, R., Nuth, C., Kääb, A., Girod, L., 2017. The effects of void handling on geodetic mass balances. In: EGU General Assembly Conference Abstracts, p. 7570.

McNabb, R., Nuth, C., Kääb, A., Girod, L., 2019a. Sensitivity of glacier volume change estimation to DEM void interpolation. Cryosphere 13 (3).

McNabb, R., Nuth, C., Kääb, A., Girod, L., 2019b. Sensitivity of glacier volume change estimation to DEM void interpolation. Cryosphere 13 (3), 895–910.

Noël, B., van de Berg, W.J., Lhermitte, S., Wouters, B., Machguth, H., Howat, I., Citterio, M., Moholdt, G., Lenaerts, J.T., van den Broeke, M.R., 2017. A tipping point in refreezing accelerates mass loss of Greenland's glaciers and ice caps. Nat. Commun. 8, 14730.

Noh, M.J., Howat, I.M., 2015. Automated stereo-photogrammetric DEM generation at high latitudes: Surface Extraction with TIN-based Search-space Minimization (SETSM) validation and demonstration over glaciated regions. GISci. Remote Sens. 52 (2), 198–217.

Nuth, C., Kääb, A., 2011. Co-registration and bias corrections of satellite elevation data sets for quantifying glacier thickness change. Cryosphere 5 (1), 271–290.

Pellitero, R., Rea, B.R., Spagnolo, M., Bakke, J., Hughes, P., Ivy-Ochs, S., Lukas, S., Ribolini, A., 2015. A GIS tool for automatic calculation of glacier equilibrium-line altitudes. Comput. Geosci. 82, 55–62.

Pfeffer, W.T., Arendt, A.A., Bliss, A., Bolch, T., Cogley, J.G., Gardner, A.S., Hagen, J.O., Hock, R., Kaser, G., Kienholz, C., Miles, E.S., Moholdt, G., Molg, N., Paul, F., Radic, V., Rastner, P., Raup, B.H., Rich, J., Sharp, M.J., Andeassen, L.M., Bajracharya, S., Barrand, N.E., Beedle, M.J., Berthier, E., Bhambri, R., Brown, I., Burgess, D.O., Burgess, E.W., Cawkwell, F., Chinn, T., Copland, L., Cullen, N.J., Davies, B., De Angelis, H., Fountain, A.G., Frey, H., Giffen, B.A., Glasser, N.F., Gurney, S.D., Hagg, W., Hall, D.K., Haritashya, U.K., Hartmann, G., Herreid, S., Howat, I., Jiskoot, H., Khromova, T.E., Klein, A., Kohler, J., Konig, M., Kriegel, D., Kutuzov, S., Lavrentiev, I., Le Bris, R., Li, X., Manley, W.F., Mayer, C., Menounos, B., Mercer, A., Mool, P., Negrete, A., Nosenko, G., Nuth, C., Osmonov, A., Pettersson, P., Racoviteanu, A., Ranzi, R., Sarikaya, M.A., Schneider, C., Sigurdsson, O., Sirguey, P., Stokes, C.R., Wheate, R., Wolken, G.J., Wu, L.Z., Wyatt, F.R., Consortium, R, 2014. The Randolph Glacier Inventory: a globally complete invento-ry of glaciers. J. Glaciol. 60 (221), 537–552.

Pithan, F., Mauritsen, T., 2014. Arctic amplification dominated by temperature feedbacks in contemporary climate models. Nat. Geosci. 7 (3), 181–184.

Pittock, A.B., 2012. Ten reasons why climate change may be more severe than projected. In: Sudden and Disruptive Climate Change. Routledge, pp. 26–42.

Porter, Claire, et al., 2023. ArcticDEM, Version 4.1 https://doi.org/10.7910/DVN/3VDC4W, Harvard Dataverse, V1, [last accessed June 2023].

Pronk, J.B., Bolch, T., King, O., Wouters, B., Benn, D.I., 2021. Contrasting surface velocities between lake-and land-terminating glaciers in the Himalayan region. Cryosphere 15 (12), 5577–5599.

Raper, S.C., Braithwaite, R.J., 2006. Low Sea level rise projections from mountain glaciers and icecaps un-der global warming. Nature 439 (7074), 311–313.

Rastner, P., Bolch, T., Molg, N., Machguth, H., Le Bris, R., Paul, F., 2012. The first complete inventory of the local glaciers and ice caps on Greenland. Cryosphere 6 (6), 1483–1495.

Rea, B.R., 2009. Defining modern day Area-Altitude Balance Ratios (AABRs) and their use in glacier-climate reconstructions. Quat. Sci. Rev. 28 (3–4), 237–248.

RGI Consortium, 2017. Randolph Glacier Inventory – A Dataset of Global Glacier Outlines: Version 6.0: Technical Report, Global Land Ice Measurements from Space. Colorado, USA.

Rignot, E., Box, J.E., Burgess, E., Hanna, E., 2008. Mass balance of the Greenland ice sheet from 1958 to 2007. Geophys. Res. Lett. 35 (20).

Rignot, E., Fenty, I., Xu, Y., Cai, C., Kemp, C., 2015. Undercutting of marine-terminating glaciers in West Greenland. Geophys. Res. Lett. 42 (14), 5909–5917.

Rounce, D.R., Hock, R., Maussion, F., Hugonnet, R., Kochtitzky, W., Huss, M., Berthier, E., Brinkerhoff, D., Compagno, L., Copland, L., Farinotti, D., 2023. Global glacier change in the 21st century: every increase in temperature matters. Science 379 (6627), 78–83.

Russo, S., Dosio, A., Graversen, R.G., Sillmann, J., Carrao, H., Dunbar, M.B., Singleton, A., Montagna, P., Bar-bola, P., Vogt, J.V., 2014. Magnitude of extreme heat waves in present climate and their projection in a warming world. J. Geophys. Res.-Atmos. 119 (22), 12500–12512.

Ryan, J.C., Hubbard, A., Stibal, M., Irvine-Fynn, T.D., Cook, J., Smith, L.C., Cameron, K., Box, J., 2018. Dark zone of the Greenland Ice Sheet controlled by distributed biologically-active impurities. Nat. Commun. 9 (1), 1065.

Scherler, D., Wulf, H., Gorelick, N., 2018. Global assessment of supraglacial debris-cover extents. Geophys. Res. Lett. 45 (21), 11–798.

Screen, J.A., Simmonds, I., 2010a. Increasing fall-winter energy loss from the Arctic Ocean and its role in Arctic temperature amplification. Geophys. Res. Lett. 37.

Screen, J.A., Simmonds, I., 2010b. The central role of diminishing sea ice in recent Arctic temperature amplification. Nature 464 (7293), 1334–1337.

Seehaus, T., Morgenshtern, V.I., Hübner, F., Bänsch, E., Braun, M.H., 2020. Novel techniques for void filling in glacier elevation change data sets. Remote Sens. 12 (23), 3917.

Serreze, M.C., Barry, R.G., 2011. Processes and impacts of Arctic amplification: A research synthesis. Glob. Planet. Chang. 77 (1–2), 85–96.

Shean, D.E., Alexandrov, O., Moratto, Z.M., Smith, B.E., Joughin, I.R., Porter, C., Morin, P., 2016. An auto-mated, open-source pipeline for mass production of digital elevation models (DEMs) from very-high-resolution commercial stereo satellite imagery. ISPRS J. Photogramm. Remote Sens. 116, 101–117.

Shepherd, A., Ivins, E., Rignot, E., Smith, B., van den Broeke, M., Velicogna, I., Whitehouse, P., Briggs, K., Joughin, I., Krinner, G., Nowicki, S., Payne, T., Scambos, T., Schlegel, N., A, G., Agosta, C., Ahlstrøm, A., Babonis, G., Barletta, V.R., Bjørk, A.A., Blazquez, A., Bonin, J., Colgan, W., Csatho, B., Cullather, R., Eng-dahl, M.E., Felikson, D., Fettweis, X., Forsberg, R., Hogg, A.E., Gallee, H., Gardner, A., Gilbert, L., Gour-melen, N., Groh, A., Gunter, B., Hanna, E., Harig, C., Helm, V., Horvath, A., Horwath, M., Khan, S., Kjeld-sen, K.K., Konrad, H., Langen, P. L., Lecavalier, B., Loomis, B., Luthcke, S., McMillan, M., Melini, D., Mernild, S., Mohajerani, Y., Moore, P., Mottram, R., Mouginot, J., Moyano, G., Muir, A., Nagler, T., Nield, G., Nilsson, J., Noël, B., Otosaka, I., Pattle, M.E., Peltier, W.R., Pie, N., Rietbroek, R., Rott, H., Sandberg Sørensen, L., Sasgen, I., Save, H., Scheuchl, B., Schrama, E., Schröder, L., Seo, K.W., Simonsen, S.B., Slater, T., Spada, G., Sutterley, T., Talpe, M., Tarasov, L., van de Berg, W.J., van der Wal, W., van Wessem, M., Vishwakarma, B.D., Wiese, D., Wilton, D., Wagner, T., Wouters, B., Wuite, J., 2020. Mass balance of the Greenland Ice Sheet from 1992 to 2018. Nature 579 (7798).

Shi, W., Wang, B., Tian, Y., 2014. Accuracy analysis of digital elevation model relating to spatial resolution and terrain slope by bilinear interpolation. Math. Geosci. 46, 445–481.

Shiggins, C.J., Lea, J.M., Brough, S., 2023. Automated ArcticDEM iceberg detection tool: insights into area and volume distributions, and their potential application to satellite imagery and modelling of glacier–iceberg–ocean systems. Cryosphere 17 (1), 15–32.

Smith, S.L., Holland, D.A., Longley, P.A., 2004. The importance of understanding error in lidar digital elevation models. Int. Arch. Photogram. Remote Sens. Spatial Inform. Sci. 35, 996–1001.

Sørensen, L.S., Simonsen, S.B., Forsberg, R., Khvorostovsky, K., Meister, R., Engdahl, M. E., 2018. 25 years of elevation changes of the Greenland Ice Sheet from ERS, Envisat, and CryoSat-2 radar altimetry. Earth Planet. Sci. Lett. 495, 234–241.

Sutherland, J.L., Carrivick, J.L., Gandy, N., Shulmeister, J., Quincey, D.J., Cornford, S.L., 2020. Proglacial lakes control glacier geometry and behavior during recession. Geophys. Res. Lett. 47 (19) p.e2020GL088865.

Takeuchi, N., Sakaki, R., Uetake, J., Nagatsuka, N., Shimada, R., Niwano, M., Aoki, T., 2018. Temporal variations of cryoconite holes and cryoconite coverage on the ablation ice surface of Qaanaaq Glacier in Northwest Greenland. Ann. Glaciol. 59 (77), 21–30.

Truffer, M., Kääb, A., Harrison, W.D., Osipova, G.B., Nosenko, G.A., Espizua, L., Gilbert, A., Fischer, L., Huggel, C., Burns, P.A.C., 2021. Glacier surges. In: Snow and Ice-Related Hazards, Risks, and Disasters. Elsevier, pp. 417–466.

Van As, D., Andersen, M.L., Petersen, D., Fettweis, X., Van Angelen, J.H., Lenaerts, J.T. M., Van Den Broeke, M.R., Lea, J.M., Bøggild, C.E., Ahlstrøm, A.P., 2014. Increasing meltwater discharge from the Nuuk region of the Greenland ice sheet and implications for mass balance (1960–2012). J. Glaciol. 60 (220), 314–322.

von Albedyll, L., Machguth, H., Nussbaumer, S.U., Zemp, M., 2018. Elevation changes of the Holm Land Ice Cap, Northeast Greenland, from 1978 to 2012–2015, derived from high-resolution digital elevation models. Arct. Antarct. Alp. Res. 50 (1).

Wang, Y., Sugiyama, S., Bjørk, A.A., 2021. Surface elevation change of glaciers along the coast of Prudhoe land, northwestern Greenland from 1985 to 2018. J. Geophys. Res. Earth 126 (11), e2020JF006038.

Xing, Z., Chi, Z., Yang, Y., Chen, S., Huang, H., Cheng, X., Hui, F., 2020. Accuracy evaluation of four green-land digital elevation models (Dems) and assessment of river network extraction. Remote Sens. 12 (20), 3429.

Yde, J.C., Knudsen, N.T., 2005. Observations of debris-rich naled associated with a major glacier surge event, Disko Island, West Greenland. Permafr. Periglac. Process. 16 (4), 319–325.

Zemp, M., Frey, H., Gartner-Roer, I., Nussbaumer, S.U., Hoelzle, M., Paul, F., Haeberli, W., Denzinger, F., Ahl-strom, A.P., Anderson, B., Bajracharya, S., Baroni, C., Braun, L.N., Caceres, B.E., Casassa, G., Cobos, G., Davila, L.R., Granados, H.D., Demuth, M.N., Espizua, L., Fischer, A., Fujita, K., Gadek, B., Ghazanfar, A., Hagen, J.O., Holmlund, P., Karimi, N., Li, Z.Q., Pelto, M., Pitte, P., Popovnin, V.V., Portocarrero, C.A., Prinz, R., Sangewar, C.V., Severskiy, I., Sigurosson, O., Soruco, A., Usubaliev, R., Vincent, C., Correspondents, W.N., 2015. Historically unprecedented global glacier decline in the early 21st century. J. Glaciol. 61 (228), 745.

Zemp, M., Huss, M., Thibert, E., Eckert, N., McNabb, R., Huber, J., Barandun, M., Machguth, H., Nussbaumer, S.U., Gärtner-Roer, I., 2019. Global glacier mass changes and their contributions to sea-level rise from 1961 to 2016. Nature 568 (7752), 382–386.